

V.L. KALASHNIKOV<sup>1,✉</sup>  
V.G. SHCHERBITSKY<sup>2</sup>  
N.V. KULESHOV<sup>2</sup>  
S. GIRARD<sup>3</sup>  
R. MONCORGE<sup>3</sup>

# Pulse energy optimization of passively Q-switched flash-lamp pumped Er:glass laser

<sup>1</sup> Institut für Photonik, TU Wien, Gusshausstr. 27/387, 1040 Vienna, Austria

<sup>2</sup> International laser Center, 65 F. Skorina Ave., 220027 Minsk, Belarus

<sup>3</sup> Centre Interdisciplinaire de Recherche Ions Lasers (CIRIL), CNRS/SEA/ISMRA 6 Bldg. Maréchal Juin 14050 Caen Cedex, France

Received: 6 December 2001/Revised version: 5 March 2002  
Published online: 8 August 2002 • © Springer-Verlag 2002

**ABSTRACT** An approach to the energy optimization of the passively Q-switched Er:glass laser is considered. The optimization procedure is represented in the maximally verifiable and usable graphical form, which is applied to the flash-lamp pumped Er:glass laser passively Q-switched with the Co<sup>2+</sup>-doped MgAl<sub>2</sub>O<sub>4</sub> and LaMgAl<sub>11</sub>O<sub>19</sub> saturable absorbers.

PACS 42.60.G; 42.55.P,R

## 1 Introduction

Optimization of the performance of Q-switched lasers has received much attention in recent years [1–5]. In general, there are two approaches to the optimization of key laser parameters such as the output coupler and initial saturable absorber transmissions. The first method considers the rate equations describing the Q-switched laser, which result in the transcendental analytical relations between the chosen input parameters and the maximal output pulse energy and minimal pulse width. The obstacle here is the need for the additional recalculations to extract values of the optimal input parameters in the explicit form, which is appropriate for practical applications. The authors of [5] showed the second method as a step-by-step creation of a family of graphical curves reflecting the laser output characteristics versus such input parameters as the output coupler and saturable absorber transmissions. The best (optimal) value of the input parameter is determined by the visual choice between curves with a maximal output energy or minimal pulse width. In this way, it is relatively simpler for applications than the former method, but for an exact estimation of the optimum, it is necessary to go through the set of different curves.

Here we present a very simple theoretical approach, and its practical application, for optimizing a passively Q-switched Er:glass laser emitting around 1.5 μm. This “eye-safe” laser is of great interest for applications in range finding and remote sensing of the atmosphere. A lot of investigations have been conducted in the last decade to find passive Q-switchers operating at 1.5 μm [6–16]. Recently, Co<sup>2+</sup>-doped

LaMgAl<sub>11</sub>O<sub>19</sub> [17] and Co<sup>2+</sup>-doped MgAl<sub>2</sub>O<sub>4</sub> [18, 19] single crystals were shown to be the most promising, efficient and reliable saturable absorber Q-switchers for the Er:glass laser. Here we compare the theoretical predictions with experimental results obtained with these Q-switchers. The main difference to others work is our presentation of the optimization procedure in a graphical form, which is maximally verifiable and easy to use for the experimenter. The optimized parameters have an explicit form, and do not need cumbersome recalculation. This is achieved owing to operation with relative shares of intra-cavity and output loss in the net-loss. This gives a physical meaning to the optimization procedure, and allows optimization tendencies to be viewed easily.

Sections 3 and 4 discuss the theoretical approach and experimental set-up, respectively. Discussion, together with the optimization, procedure is given in Sect. 5.

## 2 Model

The model under consideration is based on that described in [2] and [4], and is formally identical to it. The following approximations were used for simplification of the analysis: (1) the relaxation from the intermediate levels to the laser level in the active medium and absorber is fast; (2) the pulse duration is much shorter than the gain medium relaxation time and longer than the cavity period; and (3) the pump rate is not sufficient to change the inversion during the generation stage. Then the pulse generation can be described on the basis of the analytically solved system of rate equations:

$$\begin{aligned} \dot{n}(t) &= -\gamma\sigma_g c\phi(t)n(t), \\ \dot{n}_0(t) &= -\sigma_{gsa}c\phi(t)n_0(t), \\ \dot{\phi}(t) &= \frac{\phi(t)}{t_{cav}} A, \\ A &= 2 [\sigma_g n(t)l_g - [\sigma_{gsa}n_0(t) - \sigma_{esa}(n_t - n_0(t))]l_a] \\ &\quad - \ln\left(\frac{1}{R}\right) - L, \end{aligned} \quad (1)$$

where  $n$  is the density of the population inversion in the gain medium,  $\phi$  is the intra-cavity photon density,  $n_0$  is the dens-

✉ Fax: +43-1/5880138799, E-mail: vladimir.kalashnikov@tuwien.ac.at

ity of the ground-level population in the absorber,  $n_t$  is the total density of the active centers in the absorber,  $\sigma_g$  is the gain cross-section,  $\sigma_{gsa}$  and  $\sigma_{esa}$  are the ground-state and excited-state absorption cross-sections in the absorber, respectively,  $l_g$  and  $l_a$  are the gain medium and absorber lengths, respectively,  $\gamma$  is the inversion reduction factor in the gain medium, which is equal to 2 for the pure three-levels medium,  $R$  is the output mirror reflectivity,  $L$  is the logarithmical linear intra-cavity loss (with the exception of the active loss in the absorber and reabsorption on the laser transition in the gain medium),  $t_{cav}$  is the cavity period, and  $c$  is the light velocity. We took into consideration the double pass of the field through the laser elements and the single reflection on the output mirror.

The change of the variable  $t$  by  $n$  in (1) allows the simple expressions for the pulse parameters [4]:

$$E = \frac{h\nu \ln\left(\frac{1}{R}\right) \ln\left(\frac{n_i}{n_f}\right)}{2\gamma\sigma_g},$$

$$P = \frac{h\nu S \ln\left(\frac{1}{R}\right) B}{\gamma t_{cav}},$$

$$B = n_i - n_m - n_{m,\infty} \ln\left(\frac{n_i}{n_m}\right) - \frac{(n_i - n_{m,\infty}) \left(1 - \left(\frac{n_m}{n_i}\right)^\alpha\right)}{\alpha}.$$

$$t_p = \frac{E}{P}. \quad (2)$$

Here  $E$ ,  $P$ , and  $t_p$  are the pulse energy, the peak power and its width, respectively;  $h$  is the Plank's constant,  $\nu$  is the frequency of the generation,  $S = \frac{\pi w_0^2}{2}$  is the Gaussian laser beam area in the gain medium ( $w_0$  is the beam radius),  $\alpha = \varrho\sigma_{gsa}/(\gamma\sigma_g)$ , and  $\varrho$  is the telescopic factor, which is equal to the ratio of the beam areas in the amplifier and absorber.

The key parameters  $n_i$  (initial inversion),  $n_m$  (inversion at the pulse maximum,  $n_{m,\infty} = \lim_{\alpha \rightarrow \infty} n_m$ ) and  $n_f$  (inversion at the end of Q-switching) can be found from the algebraic equations:

$$2\sigma_g n_m l_g = \ln\left(\frac{1}{R}\right) + \delta \ln\left(\frac{1}{T_0^2}\right) + L + (1 - \delta) \ln\left(\frac{1}{T_0^2}\right) \left(\frac{n_m}{n_i}\right)^\alpha,$$

$$2\sigma_g \alpha l_g (n_f - n_i) = \alpha \ln\left(\frac{n_f}{n_i}\right) \left[ \ln\left(\frac{1}{R}\right) + \delta \ln\left(\frac{1}{T_0^2}\right) + L \right] + \ln\left(\frac{1}{T_0^2}\right) (1 - \delta) \left[ 1 - \left(\frac{n_f}{n_i}\right)^\alpha \right],$$

$$n_i = \frac{\ln\left(\frac{1}{R}\right) + \ln\left(\frac{1}{T_0^2}\right) + L}{2\sigma_g l_g},$$

where  $\delta = \sigma_{esa}/\sigma_{gsa} = \ln(T_f)/\ln(T_0)$  is the parameter that takes into account the contribution of the excited-state absorption in the saturable absorber ( $T_0$  and  $T_f$  are the initial and fully saturated transmissions of the absorber, respectively).

The system (2)–(3) will be used for calculation of the pulse parameters in the comparison with experimental data for the finite value of  $\alpha$  (see Figs. 1 and 2). As the adjustable parameter we use  $L$ , though, of course, we have the approximate experimental estimations for this value (see the next section).

In our case (Er:glass laser with the relatively small gain cross-section  $\sigma_g = 7 \times 10^{-21} \text{ cm}^2$ ,  $\varrho \approx 1$ ,  $\sigma_{gsa} \gg \sigma_g$ ), the following approximation allows the essential simplifications:  $\alpha \rightarrow \infty$  and, as a consequence,  $n_m = n_{m,\infty}$ . Following [4], let

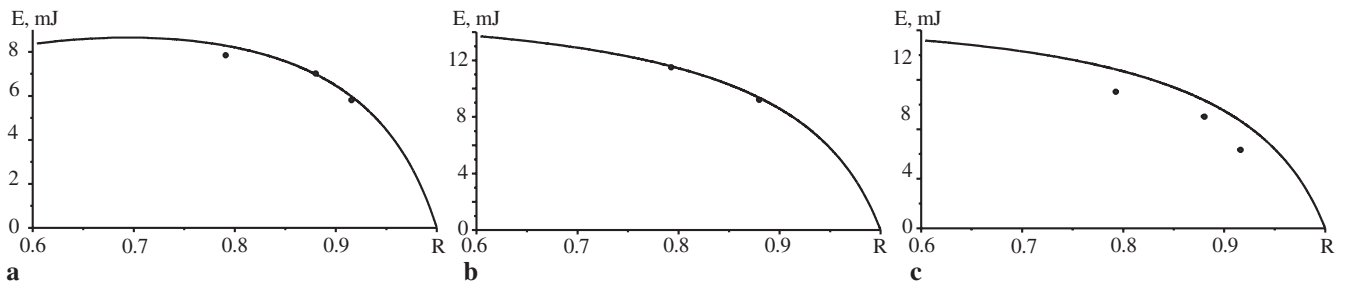


**FIGURE 1** The pulse energies versus the reflectivity of output coupler for Co:LMA (a)  $\sigma$ -polarization, (b)  $\pi$ -polarization) and Co:MALO (c) saturable absorbers (curves – theory, see (2); points – experiment).  $\delta = 0$ ,  $\alpha = 9.3$  (a), 29.4 (b), 20 (c),  $L = 6\%$

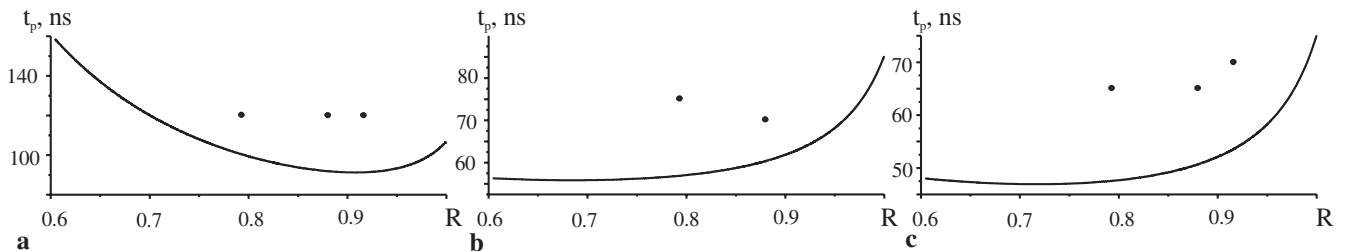


**FIGURE 2** Pulse durations versus the reflectivity of output coupler for Co:LMA (a)  $\sigma$ -polarization, (b)  $\pi$ -polarization) and Co:MALO (c) saturable absorbers (curves – theory, see (2); points – experiment). Parameters correspond to Fig. 1

us define the new variables:

$$y = \frac{n_f}{n_i}, a = \frac{\ln\left(\frac{1}{R}\right)}{2\sigma_g n_i l_g}, b = \frac{L}{2\sigma_g n_i l_g}, c = \frac{\ln\left(\frac{1}{T_0}\right)}{2\sigma_g n_i l_g},$$

$$\varepsilon = \frac{2\sigma_g E \gamma}{\aleph h \nu S}. \quad (4)$$

Since  $a + b + c = 1$ , as follows from the last equation of system (3), there is a clear physical sense of these variables:  $a$ ,  $b$ , and  $c$  are the relative shares of the output loss, the linear intracavity loss and the initial absorber's loss, respectively, in the laser's net-loss  $\aleph$ . The latter defines the lasing threshold, and is equal to  $\aleph = \ln\left(\frac{1}{R}\right) + L + \ln\left(\frac{1}{T_0}\right) = 2\sigma_g n_i l_g$ . This simple physical treatment will allow us to express the optimization procedure in the maximally verified form.

Our main goal is the optimization of the Q-switched laser performance for fixed cavity geometry and the linear intracavity loss  $L$ . We shall optimize the output pulse energy by the maximization of  $\varepsilon$  due to the variation of  $y$ . The pulse peak power and/or its width can be optimized likewise (see the second and fourth expressions of (2)), but we do not investigate this subject in detail. One can find from (2)–(3) for  $\alpha \rightarrow \infty$ :

$$y_{\text{opt}} = b + \delta(1 - b),$$

$$a_{\text{opt}} = \frac{\frac{b + \delta(1 - b) - 1}{\ln(b + \delta(1 - b))} - (1 - \delta)b - \delta}{1 - \delta}, \quad (5)$$

$$\varepsilon_{\text{max}} = \frac{(b + \delta(1 - b))(\ln(b + \delta(1 - b)) - 1) + 1}{1 - \delta}.$$

Fixation of  $L$  allows us to find  $a_{\text{opt}}$  and  $c_{\text{opt}}$ , i.e. the optimal shares of the output loss and the initial absorber's loss in the laser's net-loss  $\aleph$ , from the second equation of system (5) and the sum rule  $a + b + c = 1$ . The simple graphical presentation of the optimization procedure will be demonstrated in Sect. 5. Our calculations were carried out using the Maple 6 algebra system, and the detailed program can be found and downloaded from <http://www.geocities.com/optomapev>.

### 3 Experimental set-up and results

The flash-lamp pumped Er:glass laser operating at a 1 Hz repetition rate at 1.534  $\mu\text{m}$  with a plane-concave cavity of 310 mm in length was used for the optimization in our experiments. The high reflector ( $R > 99.5\%$  @ 1.534  $\mu\text{m}$ ) had a 2 m radius of curvature. Three different mirrors were used for output coupling, including a concave mirror with a 5 m radius of curvature and 8.4% transmission, and plane mirrors with 12% and 20.7% transmissions. The QX-7 Cr,Yb,Er-doped phosphate glass rod of  $\varnothing 3 \times 49$  mm in size from Kigre Inc. was used as the active element.

The laser was adjusted to produce the highest pulse energy in a single transverse mode with the nearly Gaussian spatial intensity distribution. The Gaussian beam shape was checked by the IR vidicon tube from Hamamatsu (model C1000) interfaced with a computer, as well as by measurement of the  $M^2$ -factor. In all cases, the intensity distribution was found to be close to the purely Gaussian profile, and the  $M^2$ -factor was approximately 1. The FWHM pulse duration and the pulse energy were measured with a fast InGaAs photodiode (rise time less than 5 ns) and a calibrated Ophir's powermeter including PE10 photosensitive head and NOVA digital display, respectively.

The laser was passively Q-switched by two kinds of saturable absorber:  $\text{Co}^{2+}$ -doped  $\text{LaMgAl}_{11}\text{O}_{19}$  (LMA) and  $\text{Co}^{2+}$ -doped spinel  $\text{MgAl}_2\text{O}_4$  (MALO) single crystals. The samples of  $\text{Co}^{2+}$ -doped LMA were provided by LETI/CEA (France). Those crystals were cut with the different orientations:  $E \parallel c$  ( $\pi$ -polarization, work position at the Brewster angle,  $\sigma_{\text{gsa}} = 4.4 \times 10^{-19} \text{ cm}^2$ ) and  $E \perp c$  ( $\sigma$ -polarization, normal to laser beam work position without antireflection coatings,  $\sigma_{\text{gsa}} = 1.4 \times 10^{-19} \text{ cm}^2$ ), where  $c$  is the crystallographic axis of LMA crystal [20]. The  $\text{Co}^{2+}$ -doped MALO disk with antireflection coatings at 1.54  $\mu\text{m}$  ( $\sigma_{\text{gsa}} = 3 \times 10^{-19} \text{ cm}^2$ ) was provided by the FEE Institution, Germany. The experimental and calculated results are shown in Table 1. The spectroscopic data were taken from [8, 13, 15], as well as defined from our saturation absorption measurements [21].

Saturable absorber	$\aleph$ , %	Theory				Experiment			
		$T_0$ , %	$R_0$ , %	$E$ , mJ	$t_p$ , ns	$T_0$ , %	$R_0$ , %	$E$ , mJ	$t_p$ , ns
Co:LMA ( $\sigma$ -polariz.) $\sigma_{\text{gsa}} = 1.4 \times 10^{-19} \text{ cm}^2$	31.5	92	91.5	6.8	110	92	91.6	5.8	120
	35.5	91	90	8.3	95	88	7	120	
	46	87.6	87.3	12.2	68	79.3	7.8	120	
Co:LMA ( $\pi$ -polariz.) $\sigma_{\text{gsa}} = 4.4 \times 10^{-19} \text{ cm}^2$	40	89.5	89	10	70	90	88	9.2	70–75
	50	86.4	86	13.8	53	79.3	11.5	75	
Co:MALO, $\sigma_{\text{gsa}} = 3 \times 10^{-19} \text{ cm}^2$	39	90	89	9.6	73	88.6	91.6	6.3	75
	43	88.6	88	11	65	88	9	70–75	
	53.4	85.3	85.5	15	50	79.3	11	70	

**TABLE 1** Optimal theoretically predicted (for  $\delta = 0$ ,  $\alpha = \infty$ ,  $L = 6\%$ ) and experimentally obtained values of Q-switching parameters for the different saturable absorbers.  $\sigma_g = 7 \times 10^{-21} \text{ cm}^2$ ,  $l_g = 4.9 \text{ cm}$

Q-switched pulses with a pulse energy of up to 11.5 mJ and a pulse width of 70 ns were shown in the experiments. A comparison with the theoretical estimations of the optimal generation parameters is presented in Sect. 4.

#### 4 Discussion

The first step is to verify the validity of the model under consideration in our specific case, and to determine  $L$  and  $\delta$ , which are required below for optimization. As shown in [21], for the chosen materials the  $\delta$ -parameter approaches zero due to the negligible excited-state absorption. First, let us compare the experimental pulse energies and durations without the optimization procedure (see Table 1) and those calculated from the system (2) (Figs. 1 and 2). We can see good agreement for energies (within the experimental error limits) and the worse agreement for durations. The under-estimation of the pulse duration is probably caused by deviation of the pulse temporal profile from Gaussian. This, as shown in [22], requires the modification of the last part of (2). However, we do not consider the pulse width minimization, and restrict ourselves to the energy maximization. Our calculations demonstrate that the best agreement with experimental energies results from  $L = 6\%$ .

The experimentally observed invariability of the pulse durations corresponds to the minimum of the pulse width dependence on  $R$  for fixed  $T_0$ , which follows from the calculations (Fig. 2), though the pulse widths are under-estimated in the model.

The verification performed above enabled us to determine the values of the parameters  $L$  and  $\delta$ . Now let us consider the next step representing the direct optimization of the output energy. As the procedure, which is appropriate for the experimental realization, we consider optimization of the output coupler and initial absorber's transmission for fixed values of the laser's net-loss  $\aleph$ . This corresponds to the fixed laser pump. The energy maximization procedure can be performed using Fig. 3. The group of curves  $a$  shows the optimal share of the output loss  $a$  in the net-loss in the dependence on the linear loss's share  $b$  for the different contributions of the excited-state absorption parameter  $\delta$ . The group of curves  $c$  is the analogous dependence for the initial absorber loss's share  $c$ .

The optimization can be performed in a simple graphical way. We have to define the laser's net-loss appropriate for our scheme, and determinate (measure or calculate) the intracavity linear loss  $L$ . That gives a value of  $b = L/\aleph$ . In Fig. 3, the vertical line corresponds to  $L = 6\%$  for a 50% net-loss, for example. The intersection with curve  $c$  (the value of  $\delta$  has to be defined, too) gives the value of optimal  $c = \ln(1/T_0^2)/\aleph$ . In our case this results in  $T_0 = 86.4\%$  (if  $\delta = \sigma_{\text{esa}}/\sigma_{\text{gsa}} = 0$ ). The intersection with curve  $a$  (for defined  $\delta$ ) gives the value of optimal  $a = \ln(1/R)/\aleph$ . For our example, this is  $R = 86\%$ . So, this procedure produces an easy and demonstrative method of Q-switching optimization. Note that curves  $a$  have a broad plateau around the parameters in question, i.e.  $a_{\text{opt}} \approx 0.296$  and  $R_{\text{opt}} \approx \exp(-0.296\aleph)$  for  $\delta = 0$  and  $\alpha = \infty$ .

The results of the pulse energy optimization are summarized in Table 1. It is important to note that each row

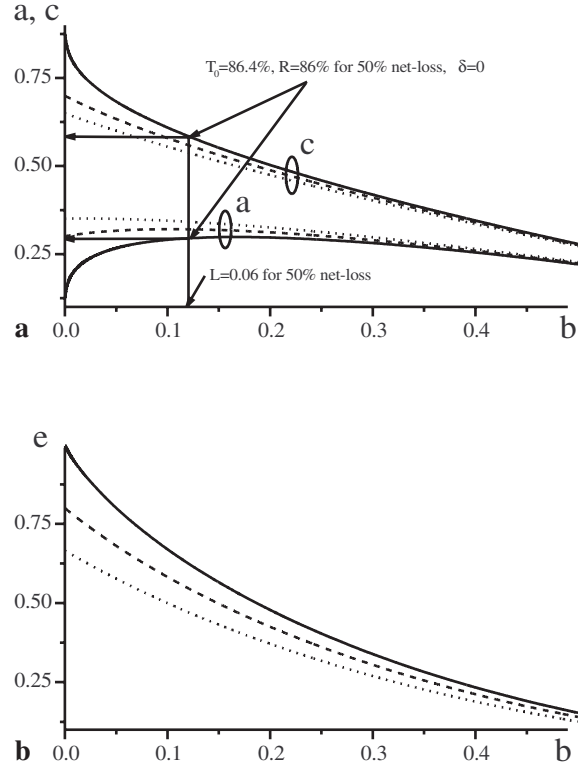


**FIGURE 3** **a** Optimal output coupling ( $a$ -curves), initial saturable loss ( $c$ -curves), and **b** dimensionless pulse energy versus linear loss parameter  $b$ . Solid, dashed and dotted curves correspond to the values of  $\delta = \sigma_{\text{esa}}/\sigma_{\text{gsa}} = 0, 0.07, 0.14$ , respectively. Horizontal and vertical straight solid lines are the utility lines for determination of the intersection points

corresponds to the fixed value of net-losses  $\aleph$ . The last row was chosen to be equal to the net-loss in the experimentally determined results from the initial transmission of the absorber and output coupler. One can see that the optimal values of  $T_0$  and  $R$  theoretically expected for  $\aleph = 31.5\%$  (Co:LMA,  $\sigma$ -polarization),  $40\%$  (Co:LMA,  $\pi$ -polarization),  $43\%$  (Co:MALO) are close to those which are tried in the experiments (see also Fig. 1). The corresponding values of the maximal energies are close (6.8 mJ and 5.8 mJ for Co:LMA ( $\sigma$ ), 10 mJ and 9.2 mJ for Co:LMA ( $\pi$ ), 11 mJ and 9 mJ for Co:MALO). The difference (less than 20%) could be explained by the calculating approximations ( $\alpha = \infty$ ,  $\delta = 0$ ) and the confinements due to the pump saturation, gain relaxation, and active crystal heating, which lie beyond the framework of our consideration. As a result of comparing the experimental data with the model predictions, the output coupler and initial absorber transmissions were not optimal for the maximal net-loss (see the last row for each absorber in Table 1). Thus, the pulse energy for the maximal net-loss could be increased by  $20 \div 56\%$ .

The main trends of the optimization procedure are obvious from Fig. 3:

1. With the increasing relative linear intracavity loss  $b$  (increasing  $L$  at fixed  $\aleph$ ), the relative optimal saturable loss  $c_{\text{opt}}$  decreases while output loss  $a_{\text{opt}}$  increases for  $b = 0 - 0.1$  or is approximately constant for  $b = 0.1 - 0.3$ .

- For the fixed value of  $L$  the relative contribution of the saturable loss  $c$  increases and that of output loss  $a$  decreases with the increasing laser net-loss  $\aleph$ . (The change of  $a$  is negligible in the interval of  $b = 0.1 - 0.3$ .)

For the above-mentioned interval of  $b$ , the output coupler's transmission is nearly proportional to  $\aleph$ :  $1 - \ln(1/R_{\text{opt}}) \approx 0.296\aleph$ .

The growth of the excited-state absorption (the transition from solid through dashed to dotted curves in Fig. 3 corresponds to  $\delta = 0, 0.07, 0.14$ , respectively) results in:

- a decrease of the relative contribution of the initial loss in the absorber;
- an increase of the relative contribution of the output loss (compare the solid, dashed and dotted curves); and
- a decrease of the pulse energy (Fig. 3b).

## 5 Conclusion

The analytical approach to the energy optimization of passively Q-switched Er:glass lasers is presented. The optimal output loss and saturable loss were shown as parametric functions of the linear loss. This gives a physical meaning to the optimization procedure, and makes it usable by the experimenter. The optimization was performed at the fixed laser's net-loss corresponding to the fixed pump level. Excited-state absorption in the saturable absorber was taken into account.

As shown, the increase in the relative contribution of the optimal saturable loss in the laser's net-loss increases the pulse energy. The decrease of the linear intra-cavity loss increases the relative contribution of the optimal saturable loss in comparison with the output loss. The excited-state absorption decreases the relative contribution of the optimal initial loss in the absorber and increases the optimal output loss.

The energy values predicted by the theory are in a good agreement with experimentally observed results for the Er:glass laser passively Q-switched by the  $\text{Co}^{2+}$ -doped  $\text{MgAl}_2\text{O}_4$  and  $\text{LaMgAl}_{11}\text{O}_{19}$  crystals.

**ACKNOWLEDGEMENTS** V.L. Kalashnikov gratefully acknowledges support from the Austrian Science Fund (FWF), Project M611. V.G. Scherbitsky express thanks to CNRS (France) for support in allowing this work to begin. The authors also thank J. Montagne from the CILAS company (France) and B. Ferrand from CEA/LETI (France) for the samples of the mirrors and LMA crystal used in given work.

## REFERENCES

- J.J. Zaykowski, P.L. Kelly: IEEE J. Quantum Electron. **QE-27**, 2220 (1991)
- J.J. Degnan: IEEE J. Quantum Electron. **QE-25**, 214 (1989)
- G. Xiao, M. Bass: IEEE J. Quantum Electron. **QE-33**, 41 (1997)
- X. Zhang, S. Zhao, Q. Wang, Q. Zhang, L. Sun, S. Zhang: IEEE J. Quantum Electron. **QE-33**, 2286 (1997)
- F.D. Patel, R.J. Beach: IEEE J. Quantum Electron. **QE-37**, 707 (2001)
- R.D. Stultz, M.B. Camargo, M. Birnbaum: J. Appl. Phys. **78**, 2959 (1995)
- M.B. Camargo, R.D. Stultz, M. Birnbaum, M. Kokta: Optics Lett. **20**, 339 (1995)
- K.V. Yumashev, I.A. Denisov, N.N. Posnov, V.P. Mikhailov, R. Moncorgé, D. Viven, B. Ferrand, Y. Guyot: J. Opt. Soc. Am. **B16**, 2189 (1999)
- T.Y. Tsai, M. Birnbaum: J. Appl. Phys. **87**, 25 (2000)
- I.A. Denisov, M.I. Demchuk, N.V. Kuleshov, K.V. Yumashev: Appl. Phys. Lett. **77**, 2455 (2000)
- A.V. Podlipensky, V.G. Shcherbitsky, N.V. Kuleshov, V.P. Mikhailov, V.I. Levchenko, V.N. Yakimovich: Optics Lett. **24**, 960 (1999)
- V.G. Savitski, A.M. Malyarevich, P.V. Prokoshin, K.V. Yumashev, E. Raaben, A.A. Zhilin: Proc. Advanced Solid-State Lasers (Seattle, WA 2001)
- K.V. Yumashev, I.A. Denisov, N.N. Posnov, V.P. Prokoshin, V.P. Mikhailov: Appl. Phys. B **70**, 179 (2000)
- Z. Burshtein, Y. Shimony, R. Feldman, V. Krupkin, A. Glushko, E. Galun: Optical Mat. **15**, 285 (2001)
- K.V. Yumashev, I.A. Denisov, N.N. Posnov, N.V. Kuleshov, R. Moncorgé: In: *Abstracts 5th Int. Conf. Excited States of Transition Elements* (Wroclaw 2001)
- B. Denker, B. Galagan, E. Godovikova, M. Meilman, V. Osiko, S. Sverchkov, I. Kertesz: In: *OSA Trends in Optics and Photonics: Vol. 26, Advanced Solid-State Lasers*, ed. by M.M. Fejer, H. Injeyan, U. Keller (OSA, WA, DC 1999)
- Ph. Thony, B. Ferrand, E. Molva: In: *OSA Trends in Optics and Photonics: Vol. 19, Advanced Solid-State Lasers*, ed. by W.R. Bosenberg, M.M. Fejer (OSA, WA, DC 1998)
- R. Wu, J.D. Myers, M.J. Myers, B.I. Denker, B.I. Galagan, S.E. Sverchkov, J.A. Hutchinson, W. Trussel: In: *OSA Trends in Optics and Photonics: Vol. 34, Advanced Solid-State Lasers*, ed. by H. Injeyan, U. Keller, Ch. Marshall (OSA, WA, DC 2000) pp. 254-256
- V.G. Shcherbitsky, A.V. Podlipensky, N.V. Kuleshov, V.I. Levchenko, V.N. Yakimovich, A. Dening, M. Mond, E. Heumann, S. Kück, G. Huber: In: *Conf. Digest Euro-CLEO/EQEC'01 Focus Meetings* (Münich, 2001)
- A. Kahn, A.M. Lejus, M. Madsac, J. Thery, D. Vivien, J.C. Bernier: J. Appl. Phys. **52**, 6864 (1981)
- V.G. Shcherbitsky, S. Girard, M. Fromager, R. Moncorgé, N.V. Kuleshov, V.I. Levchenko, V.N. Yakimovich, B. Ferrand: Appl. Phys. B (2002)
- J. Liu, D. Shen, S.-Ch. Tam, Y.-L. Lam: IEEE J. Quantum Electron. **QE-37**, 888 (2001)